

# EXPERIMENTS ON A SCALE MODEL OF A MONOLITHIC CONCRETE SPAR FOR FLOATING WIND TURBINES

**Alexis Campos**

*Universitat Politècnica de Catalunya*  
[alexis.campos@upc.edu](mailto:alexis.campos@upc.edu)

**Climent Molins**

*Universitat Politècnica de Catalunya*  
[climent.molins@upc.edu](mailto:climent.molins@upc.edu)

**Xavier Gironella**

*Universitat Politècnica de Catalunya*  
[xavi.gironella@upc.edu](mailto:xavi.gironella@upc.edu)

**Daniel Alarcón**

*Universitat Politècnica de Catalunya*  
[daniel.alarcon-fernandez@upc.edu](mailto:daniel.alarcon-fernandez@upc.edu)

**Pau Trubat**

*Universitat Politècnica de Catalunya*  
[pau.trubat.casal@upc.edu](mailto:pau.trubat.casal@upc.edu)

## Abstract

Preliminary studies of a concept consisting of a monolithic concrete SPAR platform were presented in 2014. The studies were performed in the framework of the AFOSP KIC-InnoEnergy project (Alternative Floating Platform Designs for Offshore Wind Towers using Low Cost Materials) showing significant costs reduction. The experimental phase of the project was developed during 2014.

The experiments comprised a set of hydrodynamic tests performed in the CIEM wave flume facility at the Universitat Politècnica de Catalunya (UPC), with a 1:100 scale model assuming Froude similitude. The complete experimental campaign included free decay tests, a set of 22 regular wave trains of different periods to determine the RAO's and another set of 21 regular and irregular wave trains in conjunction with a mechanical wind device, simulating the mean thrust force exerted by the wind turbine.

To adjust the weight of the whole system, a set of adjustable weights inside de scale model were designed assuring such properties, particularly the pitch/roll inertia. The scaled model of the mooring system was carefully studied because the constraints in width of the flume facility. A mechanical wind device was also specifically designed to ensure an averaged force at the top of the model, simulating the effect of the mean rotor thrust force.

A detailed description of the methodology for the experimental campaign and a summary of the experimental results are presented.

## 1. INTRODUCTION

Currently, huge efforts have been devoted on how to reduce the costs of the new floating offshore wind turbines substructures. Preliminary studies of a concept consisting of a monolithic concrete SPAR platform were presented in 2014 [1]. The studies were performed in the framework of the AFOSP KIC-InnoEnergy project (Alternative Floating Platform Designs for Offshore Wind Towers using Low Cost Materials) showing significant CAPEX and OPEX reductions[2]. The experimental phase of the project was developed during 2014.

The experimental campaign includes free decay tests, a set of 22 regular wave trains of different periods to determine the RAO's and another set of 21 regular and irregular wave trains in conjunction with a mechanical wind device, simulating the mean thrust force exerted by the wind turbine.

The paper is focused on the experimental program design, its monitoring and some of the results. Regarding the model design, it was intended to maintain all the external geometry properly scaled to be suitable for future specific experimental tests. Then, a material whose density is close to the concrete one should be selected in order to allow the adjustment of both the weight and the centre of gravity and the pitch/roll inertia. In order to correct the effect of the weight of the instruments used for monitoring or/and manufacturing imperfections between the theoretical and the manufactured mechanical properties of the scale model, a set of adjustable weights inside de scale model was designed assuring such properties, particularly the pitch/roll inertia. The exact position of the weights was finely tuned to exact fit the model properties.

The scaled model of the mooring system was carefully studied because the constraints in width of the flume facility. An optimized truncated system of catenaries was successfully used [3].

A mechanical wind device was also specifically designed to ensure a quasi-static force at the top of the model, simulating the effect of the mean rotor thrust force. The pros and cons of using this kind of simple mechanical wind device are appraised.

A detailed description of the methodology for the experimental campaign is presented, including the adjustment and checking of the final properties of the manufactured scale model, the mechanical wind device system design and configuration as well as the monitoring used during the tests. Finally, a summary of the experimental results is also presented.

## 2. MAIN OBJECTIVES

The main objectives of the AFOSP experimental campaign were:

- Obtain pitch and heave free decay experimental data.
- Obtain 6DOF motion data under regular and irregular waves and wind thrust.
- Obtain experimental RAO's

The data collected during this tests were employed for calibrating the hydrodynamic numerical tools, allowing more realistic simulations. During this experimental campaign, it was not intended to reproduce the dynamic effects of a wind turbine, then a mechanical wind device simulating a scaled mean thrust of 600kN was designed.

## 3. FACILITIES

The wave flume where the tests were carried out is the Lab of Marine Engineering at the Universtitat Politècnica de Catalunya. The CIEM [4] wave flume is 100m long, 3m wide and up to 7m deep (Figure 1). The flume is equipped with windows along its length, allowing non-intrusive optical observation techniques to be used in a wide range of experimental arrangements. The depth during the tests was set to 2.65m.

Waves and currents are generated by a wedge-type wave generator and a bidirectional pumping system whose capacity is 2000 l/s. The system is hydraulically actuated and PC-controlled, being able to produce waves up to 1.6m.

The control software allows regular and irregular waves (e.g. parametric or used-defined spectra and measured time series) to be generated.



Figure 1: Wave generator(left) and test in progress (right)

Since it was opened in 1993 many national and international projects have been developed at the facility. In 1997, it was recognized as a large-scale facility by the EU's Directorate-General for Research, and in 2006, as an outstanding science and technology installation (ICTS) by the Spanish Ministry of Science and Education.

The free decay and the mooring tests were performed in a 12x4.6m basin, with a total depth of 2.65m, Figure 2.



Figure 2: Basin for free decay and mooring tests

## 4. SCALED MODEL

The scaled model is based on the AFOSP project design [5], assuming a scale factor of  $\lambda = 100$ . From the different hydrodynamic scaling options, the Froude similitude is assumed to be the most adequate for the flume channel tests, where gravitational loads are, by far, the most relevant.

To take into account the different water density between the assumed for the prototype design ( $\rho=1,025\text{kg/m}^3$ ) and the density of the water in the flume channel ( $\rho=1,000\text{kg/m}^3$ ), a correction was made by defining the parameter  $\eta$  as the ratio between both densities, being the total weight of the system corrected by  $\eta$  to maintain the required draft [6].

The model should be appropriate for other type of tests, therefore, the floater and the tower external dimensions were properly scaled. Aluminium was chosen as the construction material for the model. This material has a similar density to the reinforced concrete ( $2500$  vs  $2700 \text{ kg/m}^3$ ), has enough resistance to the corrosion and is easy to mechanize. It is worth to note that as more similar the density between the model and the prototype, the easier the scaling of the prototype when the whole external geometry has to be scaled. The mechanization process of the structure was done in two main parts: the cylinder and the tapered tower.

Because the thickness of the model was critical for the final properties of the model, the tapered tower was mechanized in 4 different pieces, each one limited to the maximum size of the mechanization equipment. All the different parts of the tapered section were finally assembled by cold welding. The joint between the tower and the cylinder was designed to permit internal access. Then, a screwed joint was used. Similarly, a screwed joint was placed at the base of the cylinder.



Figure 3: Mechanization process

After all, the mechanization process could not match exactly the dimensions, the mass, the center of mass (CoM) and the inertia. Hence a special system for ballasting was designed to obtain an extra degree of freedom for fitting the total inertia, the mass and the

center of mass (CoM). The system was composed by two sets of several stainless steel circular plates. For a required amount of ballast weight, moving up or down both sets of plates, the CoM can be adjusted as desired, while the inertia can be tuned by separating both sets of plates from its local CoM, maintaining the system CoM.

The capacity to adjust the inertia in this way is limited to certain manufacturing tolerances, which is the reason to justify the use of aluminium against other materials with different densities.

A detail of the ballasting system, as well as a sketch of the main dimensions of the scaled model are depicted in Figure 4.

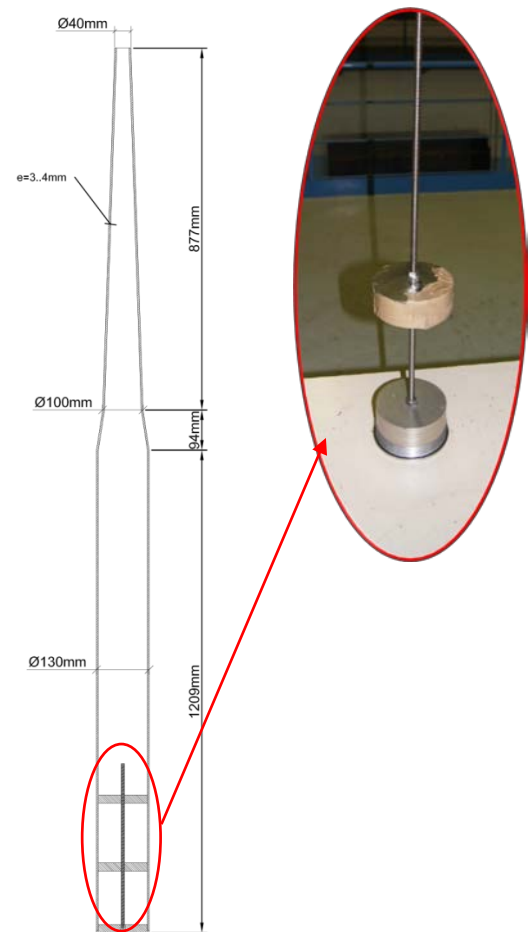


Figure 4: Scale model dimensions and ballasting system detail

Regarding the scaled model of the mooring system, the directly scaled mooring lines present a radius of  $7.27 \text{ m}$  [5] which is not compatible with the sizes of the flume, as is schematically shown in Figure 5

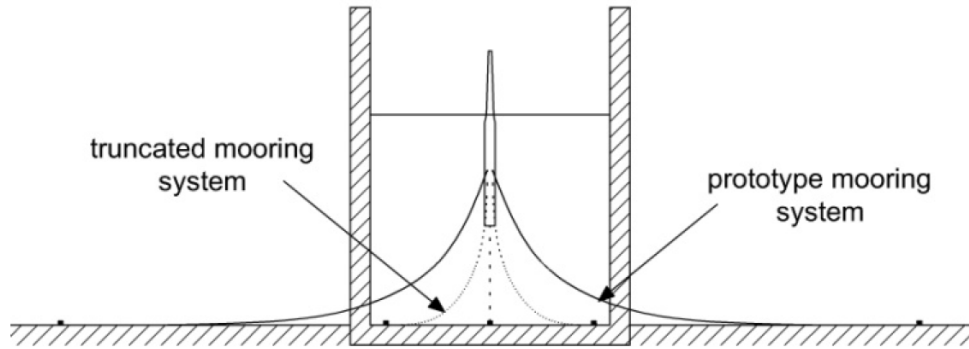


Figure 5: Prototype vs truncated mooring system

Therefore, a truncated catenaries mooring system has been designed [3]. The truncated mooring system is defined by the radius to anchor, the line length and the materials that define the different segments of the mooring line. The radius to anchor is previously defined as the maximum radius allowed by the channel width taking account the margins for the proper installation of the mooring system. Furthermore, if the truncated mooring line is composed of a unique cross section, the necessary weight to achieve the restoring forces of the prototype system would cause huge vertical forces on the floating platform. For this reason two different chain sections were chosen for designing the mooring line. The heaviest line section is positioned at the bottom, connected to the anchor, and provides the restoring horizontal force. The upper section, a light segment connected to the platform, reduces the total line weight due to its low weight. The exact properties of the lines are obtained through an optimization problem to fit the responses between the prototype mooring system and the truncated one. A detail of the mooring setup is shown in Figure 8. The complete mooring system was defined by 3 different lines, placed symmetrically at 120°. The fairleads were placed at 60cm from the bottom of the structure.

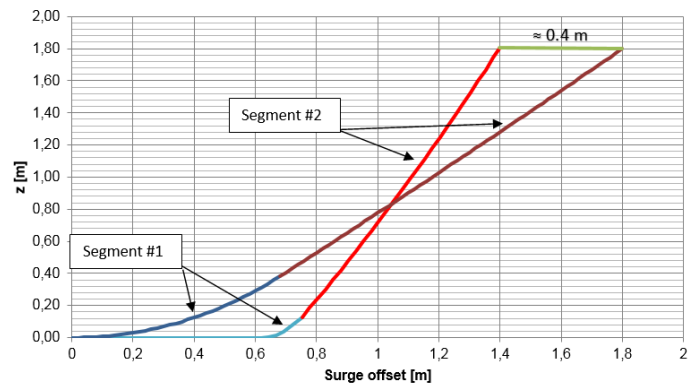


Figure 7: Mooring line shape for two different offsets

Figure 7 shows the catenary line shape in the initial position and the shape at the maximum offset for no uplifting reaction on the anchor (0.4m). Segment #1 is the lighter segment, segment #2 the heaviest one. The mooring lines properties are shown in Table 1.

Segment	#1	#2
Length [m]	0.8	1.95
Mass [g/m]	226.31	7.05

Table 1: Mooring lines properties

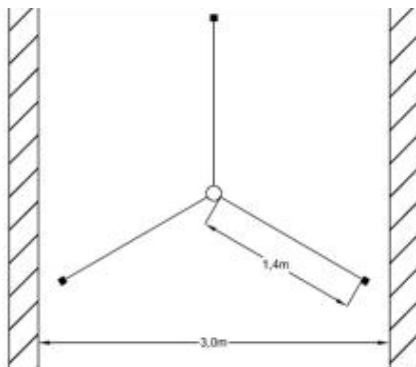


Figure 6: Plan view of the mooring system set-up



Figure 8: Detail of the mooring system setup

## 5. PHYSICAL PROPERTIES

The determination of the physical properties of the system is crucial to assure the correct weight, the CoM and the inertia. The process implies several iterations, adjusting the ballast system until the desired properties are reached.

While the measurement of the external dimensions, the total weight and the position of the CoM are not difficult tasks, the procedure for determination the pitch/roll inertia is explained in the following lines, being more complex than the other parameters.

### 5.1. Moment of inertia

The easiest way to measure the rotational inertia on the CM of the model is by inducing free oscillations around a specific axis while measuring the angular motion with a potentiometer attached to it, Figure 9.

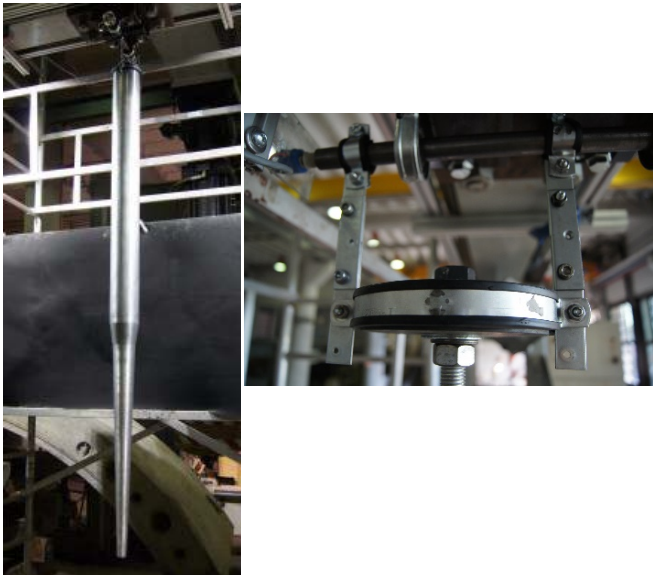


Figure 9: Pendulum test (left) Detail of the rotation axis and instrumentation (right)

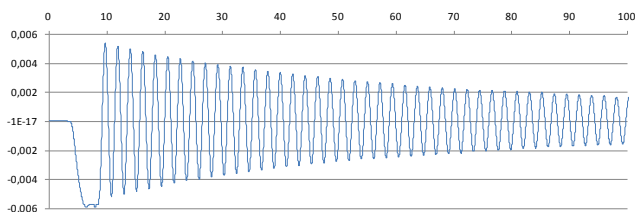


Figure 10: Angular displacement vs time

The moment of inertia can be derived from measuring the period of the oscillation from the collected data, Figure 10. This inertia corresponds to the axis from where the model is oscillating. To obtain the inertia from CoM it is necessary to apply the parallel axis theorem, translating the inertia to the CoM axis.

Assuming small amplitudes, the equation of motion is defined by (1), from where the inertia can be correlated

to the oscillation period by (2) , where  $\overline{CM}$  is the distance from the CoM to the rotation axis, m the mass, g the gravity, T the period,  $I_0$  the moment of inertia respect the rotation axis and  $\theta$  the angular motion :

$$\overline{CM} \cdot m \cdot g \cdot \theta = I_0 \ddot{\theta} \quad (1)$$

$$I_0 = \left( \frac{T}{2\pi} \right)^2 \overline{CM} \cdot g \cdot m \quad (2)$$

## 6. MONITORING

The monitoring system used in the experimental campaign was composed by wave height sensors, an inertial sensor and an IR tracking system.

- **Wave height sensor:** Composed by a resistance sensor, Figure 11, placed at the same longitudinal position as the structure to obtain the water surface position. Its sampling rate was 40Hz.

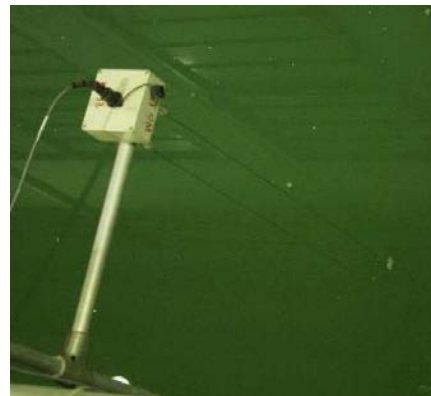


Figure 11: Wave height sensor

- **Inertial sensor:** As secondary monitoring device, the 6 dof inertial sensor, Figure 12, was placed inside the nacelle, obtaining the local accelerations. This sensor has a sampling rate of 128Hz.



Figure 12: Inertial sensor

- **IR tracking system:** The main monitoring device used for the tests. Was a 6 DOF IR optical tracking system, capable to compute the 3 dimensional coordinates of the selected points with accuracy about 1mm. The inclinations are computed from a set of points placed at the top of the nacelle as a rigid body (Figure 13). The capture of the motions was done at 120 Hz.

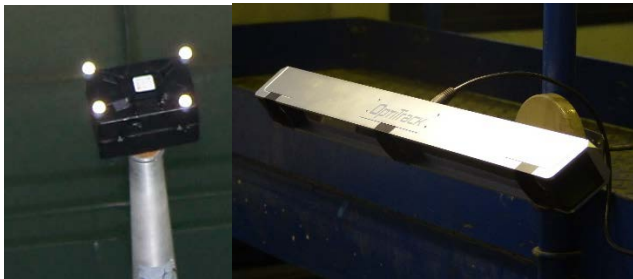


**Figure 13: IR tracking system. Markers on the nacelle (left). IR cameras (right)**

- Finest control of the force actuating over the model.
- Low cost of the equipment involved.
- Reasonable developing time.
- Easy set-up on the wave flume.

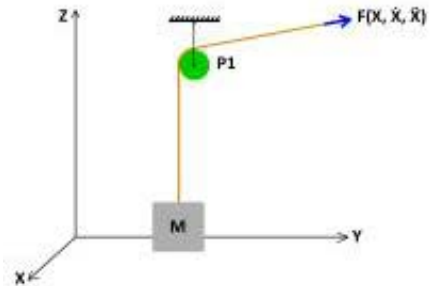


**Figure 14: Sketch of the wind device system**

The wind device system was fixed to an external frame (Figure 15), installed around the structure and large enough to not interfere with the expected motions during the tests. The device (Figure 16) was capable to be placed in several positions along the frame, being possible to apply the wind force from almost all possible relative directions against waves.

## 7. WIND DEVICE

The loads generated by the wind turbine in the experimental campaign are applied by a pulley system. This simple device does not take into account the wind profile neither the controlling method, which are very difficult to be reproduced on a scaled model [7]. On the other hand, the static force applied on the top of the nacelle to simulate the FOWT mean force is enough to represent the main load transferred from the FOWT to the platform, the thrust of the wind.

The wind device is basically composed by a nylon pulley and a weight tied to the line that actuates on the top of the model, Figure 14. The selected pulley has almost negligible mass and inertia, in order to avoid dynamic damping and other interferences. A nylon line is selected to link the weight and the nacelle. The nylon density is small enough to avoid slacks on the rope while the platform oscillates, being its mass negligible as well as the pulley's, which contributes to avoid temporal variation of the force and damping to the system. Despite being these effects almost negligible, they were measured in order to quantify its effect. The static frictional moment has been obtained in the lab measuring the incremental force applied on the pulley that reaches the movement of the bearing. On the other hand, since the dynamic frictional moment is difficult to obtain, the manufacturer recommendation is assuming the dynamic frictional moment as half of the value of the static one.

The main design criterion of the pulley system is the application of a given force as much constant as possible while the platform is moving in the water. The main criteria followed to design the mechanical system were:



**Figure 15: Wind device external frame setup**

e



**Figure 16: Detail of the wind device**

## 8. MOORING SYSTEM TESTS

The mooring lines restoring forces were experimentally determined with a set of specific tests designed to obtain the response of the mooring system used in the hydrodynamic tests. Those results were analysed and validated with the analytical predictions of the mooring system. The test was performed in dry conditions with a frame that contributes to maintain the constant height (Figure 18) and a rail with a trolley that allow a free movement in one direction on the horizontal plane of the fairleads (Figure 19). Therefore the restoring force of the catenary line or system in the free movement direction is evaluated by applying a known destabilizing force. A sketch of the test is shown in Figure 17.

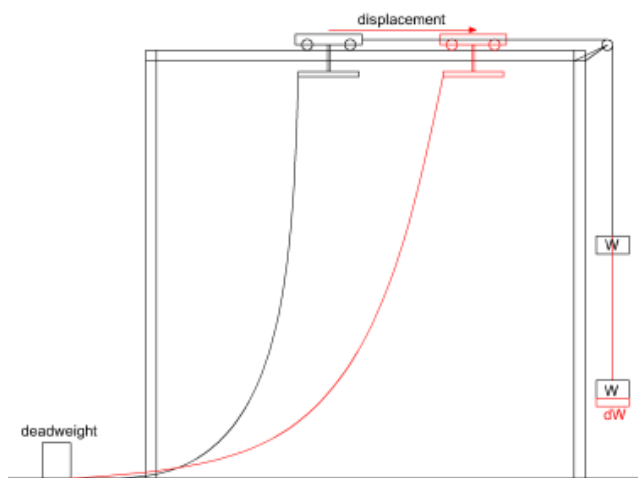


Figure 17: Mooring line test sketch

The tests were carried out both for a single catenary line, and a catenary system in two directions. Figure 20 shows the comparison between the experimental data and the numerical predictions for the horizontal response of a single catenary line. In general, the results perfectly fit the numerical predictions, but for the smallest values of  $x$  motion, some differences are apparent due to the friction of the external testing devices.



Figure 18: Mooring tests frame

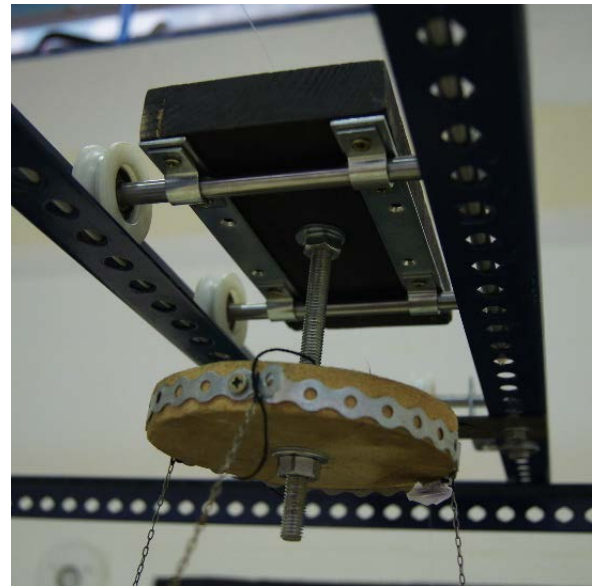


Figure 19: Detail of the trolley

Figure 21 shows the catenary line response in  $x$  direction ( $F_x$ ) for a constant  $y = 30 \text{ cm}$ , and in  $y$  direction ( $F_y$ ) for a constant  $x = 0 \text{ cm}$  respectively. The results show that the response of the catenary system matches successfully with the geometric composition of each line restoring force.

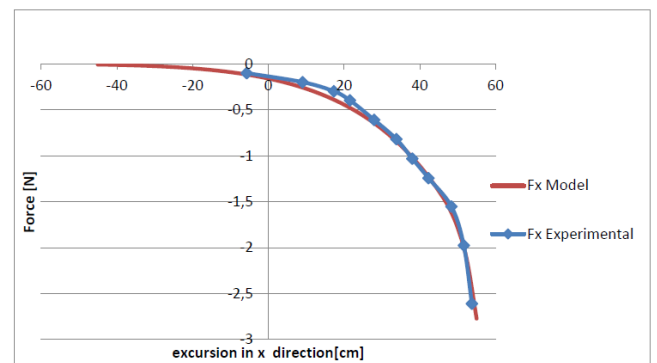


Figure 20: Single catenary test vs numerical model

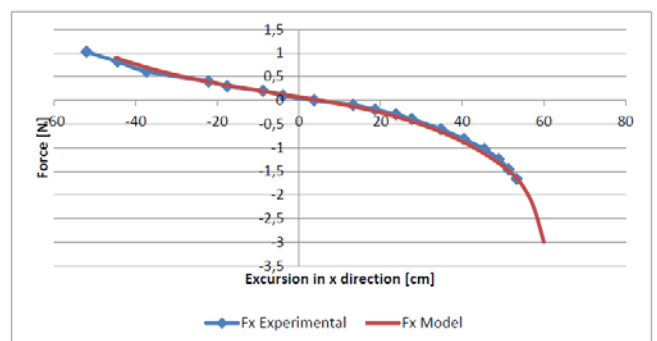


Figure 21: Mooring system test vs numerical model

## 9. FREE DECAY TESTS

To experimentally obtain the eigenperiods of the heave and pitch/roll motions, as well as its damping, a set of free decay tests were performed in the basin. The tests include the free floating and the moored situations. In the case of yaw motion, only the free decay test in the moored situation was performed.

### 9.1. Heave free decay

The heave free decay test is the simplest one to setup, lifting up the structure up to 10cm above the waterline from its equilibrium position to be later released. The lifting is done with a manual crank linked to a nylon thread, which is attached to nacelle of the structure as is schematically shown in Figure 22. A picture of the test is shown in Figure 23.

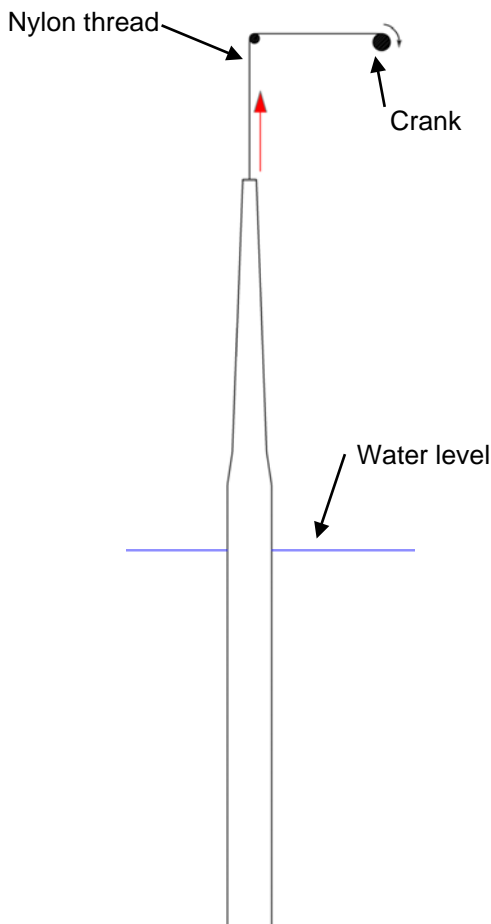


Figure 22: Sketch of the heave free decay setup

To minimize perturbations of other motions than the heave one, the structure was in rest at the lifted position for several minutes before releasing the structure.



Figure 23: Heave free decay

### 9.2. Pitch/roll free decay

The pitch/roll free decay test presents one of the most challenging setups to assure an isolated motion in that direction. Figure 24 shows a sketch of the setup to impose an initial inclined condition. In that case a set of two nylon threads was used to apply a pair of forces over the structure. Both ends of the nylon threads were simultaneously rolled with a manual crank, being possible to fix the crank at the desired position and wait until the structure rest in equilibrium. Similarly to the heave free decay test, once the nylon threads are released, the system starts to oscillate in pitch direction, with a very reduced surge motion due to the initial conditions. A picture of the pitch/roll free decay is shown in Figure 25. Different bars fixed to an external frame were used to change the thread direction as required.

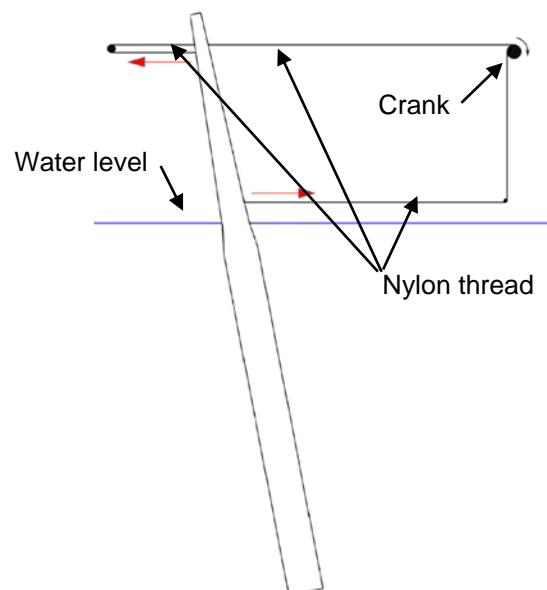


Figure 24: Sketch of the pitch/roll free decay setup

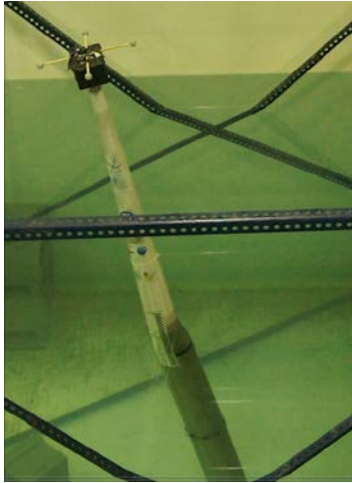


Figure 25: Pitch/roll free decay

### 9.3. Yaw free decay

The yaw free decay setup was a variant of the pitch/roll free decay test. In this case, the two nylon threads are connected to the tower base, in a diametrically opposite configuration. By rolling both ends of the threads with a manual crank, the initial condition for yaw motion was fixed.

## 10. RAO TESTS

A set of 21 frequencies of regular wave trains were produced in order to determine experimentally the RAO's of the structure, including the effect of the mooring system. Since it is not possible to reproduce waves of 1cm height in the wave flume, the wave height for each test was set around 5cm. A picture of the scale model setup is shown in Figure 26.



Figure 26: Scale model setup at the wave flume.

For both the free decay and the RAO's test, the eigenperiods coincides in  $T=3s$  for heave and  $T=4s$  for pitch.

## 11. WIND & WAVE TESTS

A set of 4 different static wind direction positions combined with 8 different type of regular and irregular waves have been applied over the structure moored at the flume bed in 2 different positions.

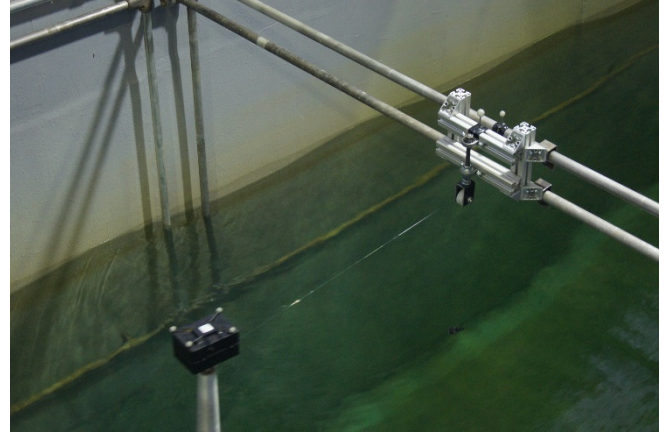


Figure 27: Detail of a test including wind device

REGULAR WAVES				
Mooring Dir.	Wind dir. [°]	T [s]	H [cm]	Pitch [°]
1	83.9	1.2	9.1	$-0.2 \pm 1.3$
	83.4	1.8	18.5	$-0.2 \pm 3.1$
	178.6	0.9	7.2	$-3.0 \pm 0.6$
	179.0	1.2	9.6	$-3.0 \pm 1.2$
	179.0	1.5	14.0	$-3.0 \pm 2.4$
	179.1	1.8	18.7	$-3.0 \pm 3.2$
2	1.2	1.2	9.3	$2.8 \pm 1.2$
	1.1	1.5	14.5	$2.8 \pm 2.0$
	1.1	1.8	18.8	$2.9 \pm 3.0$
	0.9	2.3	28.5	$2.9 \pm 5.2$
	25.4	0.9	6.6	$3.0 \pm 0.9$
	25.6	1.2	9.5	$2.9 \pm 1.1$
	25.6	1.5	14.1	$2.9 \pm 2.0$
	25.7	1.8	18.7	$2.9 \pm 2.9$
IRREGULAR WAVES				
Mooring Dir. <sup>1</sup>	Wind Dir. [°]	T <sub>P</sub> [s]	H <sub>s</sub> [cm]	Pitch [°]
1	84.2	0.9	5.1	$-0.3 \pm 1.2$
	179.0	0.9	4.9	$-3.0 \pm 0.9$
	179.0	1.8	21.4	$-2.9 \pm 5.2$
2	1.4	0.9	5.1	$2.9 \pm 1.2$
	1.4	1.8	21.2	$2.8 \pm 7.2$
	25.6	0.9	5.2	$3.0 \pm 1.8$
	25.5	1.8	15.9	$3.0 \pm 6.1$

Table 2: Summary of wind-wave tests performed

Table 2 summarizes the tests performed during the experimental campaign. Wind direction refers to the misalignment of the wind direction against waves, being 0 when they are aligned. T and  $T_p$  refers to the period or peak period of the wave train and H is the height. Also the measured maximum range of the pitch motion for each test is included. Mooring direction corresponds to: Position #1: Mooring line aligned with the flume placed downstream. Position #2 Mooring line aligned with the flume placed upstream.

## 12. CONCLUSIONS

A detailed description of the methodology of the experimental campaign developed during AFOSP project has been presented, including the checking of the real properties of the manufactured scale model, the mechanical wind device system design as well as the monitoring used during the tests.

The experimental campaign was successful and all the required hydrodynamic parameters to calibrate the numerical models used in subsequent simulations were obtained.

The mechanical device to simulate a mean thrust force was useful to test the structure under operational inclinations while the stiffness of the moorings is increased by the excursion of the platform because of the wind force. Nevertheless, its application is limited to this, being not possible to reproduce the dynamic effects of the wind turbine, wind gusts or turbulence.

Finally, some of the experimental results have been presented in the paper.

## 13. ACKNOWLEDGMENTS

The experimental campaign presented in this paper was developed under the framework of the KIC Innoenergy (EIT) AFOSP innovation project (Alternative Floating Offshore Support Platform), which financial support is greatly appreciated. Also the contribution of the other members of the consortium: Gas Natural Fenosa and the University of Stuttgart is really appreciated.

## REFERENCES

- [1] Matha, D; Sandner, F; Molins, C; Campos, A; Cheng,P., "Efficient preliminary floating offshore wind turbine design and testing methodologies and application to a concrete spar design," *Philos. Trans. A*, 2015.
- [2] Molins,C.;Campos,A.;Sandner,F.;and Matha,D., "Monolithic concrete off-shore floating structure for wind turbines" in *EWEA 2014 Barcelona*, 2014, pp. 107–111.
- [3] Molins,C.;Trubat,P.;Gironella,X.;and Campos,A., "Design optimization for a truncated catenary mooring system for scale model test" in *Offshore Renewable Energy ORE2014*, 2014.
- [4] CIEM/LIM, "UPC ICTS-CIEM/LIM (Maritime Research and Experimentation Wave Flume)." Barcelona.
- [5] Molins,C.;Matha,D.;Sandner,F.;Campos,A.;Trubat,P.;and Roca,P., "AFOSP WP2: Prototype Conceptual Design. D2.2 Prototype pre-design," 2013.
- [6] Chakrabarti,S., *Handbook of offshore engineering Vol 1 & 2*. Elsevier, 2005.
- [7] Otto,W. and Huijs,F., "Development of a Scaled-Down Floating Wind Turbine for Offshore Basin Testing," in *Proceedings of the ASME 2014 33rd International Conference on Ocean, Offshore and Arctic Engineering (OMAE2014)*, 2014, pp. 1–11.